PHYSICAL REVIEW B
CONDENSED MATTER

THIRD SERIES, VOLUME 51, NUMBER 2 1 JANUARY 1995-II

Ionization energy for charged particles in Ge

S. Y. Tong* and W. N. Lennard
Department of Physics, The University of Western Ontario, London, Ontario, Canada N6A 3K7
(Received 9 May 1994)

The response of a hyperpure Ge detector (volume ~ 0.7 cm^3) to ionizing radiation has been studied with regard to the radiation ionization energy ratio, $\varepsilon_{\text{ion}}/\varepsilon_0$, using radioactive (α,γ) sources and accelerated ion beams (^{1}H,^{4}He). These data provide evidence that ε_{ion} is *not* identically equal to ε_0 for low-energy (e.g., few MeV) charged particles, in qualitative accord with data for Si detectors. The apparent thickness of the ion-implanted entrance window of the detector exhibits a marked dependence on temperature in the region 80–183 K. As well, channeling effects have been observed which can be attributed to residual crystalline structure in this inactive layer.

I. INTRODUCTION

The principal characteristic describing the response of semiconductor detectors to ionizing radiation is the mean energy to create electron-hole pairs, denoted by ε. Since ε is known to vary with the type of radiation for Si (Ref. 1 and references therein), its value is specified by ε_0, ε_{e-}, ε_p, ε_d, ε_α, etc., corresponding to photons, electrons, protons (^{1}H), deuterons (^{2}H), alphas (^{4}He), etc., respectively. All available experimental data have confirmed that $\varepsilon_0 \equiv \varepsilon_{e-}$ for both Si and Ge; in both these cases, a comparatively diffuse plasma of electrons and holes is produced. However, extensive careful measurements spanning two decades have shown that $\varepsilon_{\text{ion}} < \varepsilon_0$ for light ions $(p,d,\alpha,\ldots)$ in Si. In fact, the response of Si detectors to charged particles has been described using a semiempirical energy dependent ε_{ion}, viz. $\varepsilon_{\text{ion}} = \varepsilon_0 - kS_e$,[1] where S_e is the electronic stopping power $(S_e \equiv dE/dx > 0)$ of the specific ionization particle in the detector medium (in this case, Si) and k is a constant *independent of the ion species* for light ions, i.e., p, d, and ^{3,4}He. A dependence of the number of collected electron-hole pairs on the charged particle stopping power might have been anticipated as the columnar (charge) plasma cloud is created during the slowing down process. No deviation from this behavior has been observed for such light ions in subsequent careful measurements by both Bauer and Bortels[2] and Hösler and Darji.[3] Recent heavy-ion data in Si detectors[4] have revealed $\varepsilon_{\text{ion}}/\varepsilon_0$ values that are, however, less than unity by a few percent—a result which is not in agreement with the semiempirical description given above. As well, no evidence for plasma recombination effects were observed. Note that the semiempirical behavior described above leads to a nonlinear detector response in terms of observed pulse heights as a function of particle energy. This anomalous behavior is not to be confused with the usual effects that contribute to the so-called "pulse height defect," i.e., nuclear (nonionizing) energy loss and entrance window (or "inactive layer") effects. It is worth noting that no clear physical picture has yet emerged that is capable of explaining the Si data even qualitatively.

The situation for Ge is not so clear. Pehl *et al.*[5] concluded that ε_0, ε_p, and ε_α are the same within the $\pm 1\%$ uncertainties of their measurements. Martini *et al.*[6] measured $\varepsilon_\alpha/\varepsilon_p = 0.9989 \pm 0.0015$ and $\varepsilon_\alpha/\varepsilon_d = 0.9963 \pm 0.0035$ for 10–19 MeV particles, but do not relate their values to ε_0. Further, the latter authors have concluded that their measured values for $\varepsilon_\alpha/\varepsilon_p$ and $\varepsilon_\alpha/\varepsilon_d$ are consistent with unity within their experimental uncertainties. The measurement uncertainties in both these works would seem to preclude definitive conclusions. Additionally, data for Si have been obtained by several investigators over a wider energy region than that spanned for Ge. In light of the Si results, the observations of equal ε values in Ge for different radiation types seems surprising. More precise measurements for Ge covering a wider range of charged particle energies would appear to be warranted.

We report here extensive measurements of the relative pulse heights produced by charged particles (p,α) and γ rays in a hyperpure Ge (HPGe) detector as functions of detector temperature, electric-field strength, etc. The

particle-γ data were registered *simultaneously* to reduce systematic errors caused by electronic drifts. Effects due to entrance window and nonionizing energy losses have been explicitly considered. The results show that ε_{ion} (i.e., ε_p, ε_α) is indeed a function of particle energy over the region spanned by the data. Effects of particle channeling in the ion-implanted window have been observed. However, the large decrease in apparent entrance window thickness with increasing detector temperature remains unexplained at this time.

II. EXPERIMENT

The detector used was a mildly p-type high-purity Ge charged particle detector (EG&G Ortec, Serial No. 30-338A, Model No. GG-020-075-7) with an active area of 75 mm^2 and a maximum sensitive depth of 9.8 mm (volume ~ 0.7 cm^3). The front window of the detector was a 40 keV boron-implanted layer (^{11}B implantation dose: 10^{14} ions cm^{-2}); the back contact consisted of a 300 μm lithium diffused layer. The operating bias applied to the detector was 1 kV although total depletion was obtained for ~ 0.4 kV.

Measurements were performed in a high vacuum chamber (volume ~ 500 cm^3) containing the Ge detector assembly. The rear surface of the planar detector was tightly fastened to a massive copper mount in the form of a cooling reservoir. The detector mount system was placed on the axis of a high-precision rotary mechanism with the rotation axis passing through the front surface of the detector. This configuration provided for a *single axis* detector tilt capability for angles in the region $-50° \leq \theta \leq 50°$ (with respect to the surface normal) with a precision of $\pm 0.017°$. Two metal bellows were connected to the cooling reservoir in order to provide for fast LN_2 cooling while at the same time maintaining adequate rotation flexibility of the detector. Using a continuous flow of LN_2 through the mounting assembly, the detector could be cooled from room temperature to 80 K within 20 min. The temperature was monitored by two thermocouples—one fastened to the front surface of the detector chassis and another directly in contact with the LN_2 reservoir. Less than 0.6 K differences was found between the readings from the two thermocouples over the temperature range 80–170 K, indicating a uniform temperature distribution throughout the detector, i.e., heat loss through the signal wire and other contacts was negligible. The face of the detector was surrounded by a large LN_2-cooled cold trap which provided for substantial improvement in the local vacuum and eliminated the possibility of condensation on the Ge crystal surface. In the experiments, this trap was cooled for approximately 30 min before cooling the detector housing itself. Using a 4000 l/s cryopump, the test chamber could be evacuated to $\sim 1.3 \times 10^{-6}$ Pa.

The simplest technique for determining the effective entrance window thickness of the detector is to vary the angle of incidence of a monoenergetic charged particle beam. When the angle of incidence is θ (i.e., measured relative to the normal to the detector surface), the energy loss in the dead layer (thickness $= \Delta t$) at an incident energy E', $\Delta E_w(E',\theta)$, is given by

$$\Delta E_w(E',\theta) = \frac{dE(E')}{dx} \Delta t \sec\theta \ . \tag{1}$$

This technique has been used for both ^1H and ^4He ions to study changes in the apparent window thickness as a function of operating conditions, i.e., bias voltage and temperature.

The basic setup as described above was used for experiments with radioactive α sources. A thin circular (mixed) triple-α source with an active area ~ 5 mm^2 containing the α emitters ^{239}Pu, ^{241}Am, and ^{244}Cm ($E_\alpha = 5156.6$, 5485.6, and 5804.82 keV, respectively[7]), was positioned in front of the detector. The distance between the detector and the α source was ~ 7 cm. A variety of γ-ray sources (^{152}Eu, ^{60}Co, ^{137}Cs, ^{133}Ba, ^{54}Mn, ^{22}Na) was used for calibration purposes during the course of these measurements. For measurements using accelerated ion beams, the front port of the chamber was connected to a large vacuum vessel and associated beam line to introduce the beam through to the detector with the α source removed, but retaining the γ source.

The electronic setup for the Ge detector consisted of the HPGe detector, bias power supply, preamplifier, amplifier, multichannel analyzer, and reference test pulse generator. The charge sensitive preamp was a Model 5091 (Electron Control Corporation, eV Products Division), providing low noise [~ 0.7 keV full width at half maximum (FWHM)] for a load capacitance of 0–100 pF. The main amplifier (Ortec 572) used a shaping time of 1 μs, which yielded the best resolution; variation of this parameter in the range 0.5–4 μs produced no observable change in the relative pulse heights. The maximum pulse height for both 1.3325 MeV γ rays and test pulses close to the γ peak was reached for a shaping time of 1 μs, which should minimize the ballistic deficit[8–10] of the amplifier. (Note that ballistic deficit effects should not be important for small planar Ge detectors where variations in charge collection times are small.) Pulse pileup rejection was used throughout although total count rates were maintained $\leq 10^3$ s^{-1}. The total system resolution was ~ 3 keV for 1.4 MeV γ rays, ~ 6 keV for 1 MeV protons, and ~ 15 keV for 5.5 MeV α particles. The precision pulse generator, operated at 60 Hz, was used to relate measured pulse heights, thereby eliminating any nonlinearity in the analog-to-digital converter (ADC). The output pulse height of the pulse generator was controlled by a precision Kelvin-Varley voltage divider containing three-decade dial switches and a variety of attenuator switches. The offset of the pulse for zero dial reading was adjusted to yield zero output. The linearity of the pulse generator was confirmed for γ-ray energies from 0.1 to 1.4 MeV using three different Ge detector-preamp combinations and different pulse amplitudes with the same amplifier-ADC system, since the photopeak pulse height is known to be precisely linear with γ-ray energy in the absence of ballistic deficit effects.[11] The differential linearity of the pulser for all pulse amplitudes was found to be better than $1.5 \times 10^{-4}\%$ for both a 200 cm^3 planar HPGe spectrometer and a 92 cm^3 coaxial Ge(Li) spectrometer (resolution ~ 1.7 keV for both) at 77 K. It was

verified that the pulse height measured for γ rays was independent of the geometrical orientation of the γ-ray source with respect to the HPGe detector.

To determine precisely the positions of γ peaks and the test pulses in the calibration spectra, both peak centroids and the most probable positions determined by a near-Gaussian fitting procedure were used—no systematic difference was found between the two choices. Test pulses were placed on both sides of each γ peak and various pulse amplitudes were cycled in time during the spectrum acquisition to minimize uncertainty arising from electronic instability.

The UWO 1.7 MV Tandetron ion accelerator was used as a tunable source of energetic ions. After momentum selection, the ion beam was steered into a scattering chamber. The ion-beam direction was determined by two adjustable apertures separated by 1 m. A target holder capable of holding up to 10 samples was located in front of the scattering chamber. The target holder could be tilted about its vertical axis which passed through the surface of the targets. This holder was electrically insulated from the frame of the vacuum chamber and equipped with a secondary electron suppression plate, thereby providing for reasonably accurate beam current integration. The detector chamber was positioned at the 20° port position at the back of this chamber such that the circular HPGe detector subtended a small solid angle, $\Delta\Omega = 1.8\times10^{-3}$ msr ($\pm10\%$), with respect to the beam spot at the position of the target. The incident beam was scattered to forward directions by a self-supporting thin foil. A movable Si detector placed at the back of the scattering chamber acted as a beam flux monitor to ensure that the scattered beam intensity was low enough to avoid catastrophic damage to the Ge detector.

Two groups of targets were mounted on the target holder in the scattering chamber for different purposes: (i) thin Al (35 μg cm^{-2}), ^{13}C (12 μg cm^{-2}), and CaF_2 (74 μg cm^{-2}) targets with Ta backings and a thin ^{12}C (7.3 μg cm^{-2}) target on a silicon substrate were used to facilitate the energy calibration of the accelerator; and (ii) a thin Au self-supporting foil ($\rho t_{\mathrm{Au}} = 68$ μg cm^{-2}) and a Au-on-C self-supporting foil ($\rho t_{\mathrm{Au}} = 9.6$ μg cm^{-2} and $\rho t_{\mathrm{C}} = 11.2$ μg cm^{-2}) were used to scatter the ^{1}H and ^{4}He ions, respectively, thereby reducing the particle flux from the accelerator. For incident ^{4}He ions, the detected peaks arising due to scattering from Au and C for the Au-on-C targets were easily resolved.

A fixed Si detector located 12 cm from the beam impact point on the target at a scattering angle of 152° with respect to the beam direction was used for *in situ* Rutherford backscattering (RBS) of 1.5 MeV ^{4}He ions to measure the thickness of the scattering foil, thereby enabling a precise determination of the energy loss of ions scattered to 20° into the HPGe detector. A Si(Bi) target with a surface Bi concentration of 4.90×10^{15} atoms cm^{-2} ($\pm2\%$) was employed as a calibration RBS target.

The energy calibration of the Tandetron ion accelerator was accomplished using nuclear reactions. Two resonant nuclear reactions were routinely employed: (1) The ^{27}Al$(p,\gamma)^{28}$Si reaction with a narrow (0.1 keV) resonance at 991.9 (±0.04) keV, and (2) the ^{13}C$(p,\gamma)^{14}$N reaction with a narrow (0.077 keV) resonance at 1747.6 (±0.9) keV.[12] The accelerator was calibrated before each pulse-height experiment and was found to be unchanged (within 0.5 keV) over several months. The total calibration time required to scan both resonances was $\sim$30 min due to (i) a large detection solid angle for the 5×5 in NaI(Tl) γ-ray detector, and (ii) adequate beam current intensity (~0.4 μA). To ensure the integrity of the above two-point calibration procedure, two further measurements were made: (1) the γ yield from the ^{19}F$(p,\alpha\gamma)^{16}$O nuclear reaction at 340.46 (±0.04) keV with a width of 2.4 keV (Ref. 12) was used to confirm the calibration at low energy; (2) the broad resonance in the ^{12}C$(\alpha,\alpha)^{12}$C elastic-scattering yield at 4265±5 keV (Ref. 13) for a scattering angle of 170° was scanned to confirm the calibration at higher energies. The extrapolated energy values from the two-point calibration were in good agreement with the latter measurements within 1.0 keV for the former case and 2.5 keV for the latter.

Earlier relative measurements of ε for particle energies below 10 MeV were based on separate measurements for γ rays and particles. There, the energy losses in the entrance window and the nuclear (i.e, nonionizing) energy loss of the particles were not carefully considered. Martini *et al.*[6] measured the rate of change of the measured pulse height as a function of incident projectile energy for their high-velocity data, which then eliminates to first order the effects of nuclear and window energy losses. The method described herein is a direct comparison of the HPGe detector response to energetic particles and γ rays made simultaneously by measuring particle-γ mixed spectra accompanied by a series of reference pulses. The characteristic γ peaks in the spectra provided the energy calibration.

The energy of the incident particles that is available for electron-hole pair creation was derived using measured values for ΔE_w (energy lost in the window and/or inactive layer) and calculated values for ΔE_n (energy lost through elastic nuclear collisions), i.e.,

$$E_{\mathrm{ion}} = E_0 - \Delta E_w - \Delta E_n - \Delta E_s \ , \tag{2}$$

where E_0 is the energy of the particles incident on the detector and ΔE_s is the energy loss for α's emanating from the mixed α source ($\Delta E_s \equiv 0$ for measurements using accelerated ion beams). E_{ion} is related to N_{eh}^{ion}, the number of pairs created in the active volume of the Ge detector, via

$$E_{\mathrm{ion}} = N_{eh}^{\mathrm{ion}} \varepsilon_{\mathrm{ion}} \ . \tag{3}$$

For γ rays, the expression relating N_{eh}^{γ} and E_γ is

$$E_\gamma = N_{eh}^{\gamma} \varepsilon_0 \ . \tag{4}$$

Both N_{eh}^{ion} and N_{eh}^{γ} are proportional to measured pulse heights. Thus the value for $\varepsilon_{\mathrm{ion}}/\varepsilon_0$ was then deduced for the same pulse heights, i.e., for $N_{eh}^{\mathrm{ion}} = N_{eh}^{\gamma}$, via

$$\frac{\varepsilon_{\mathrm{ion}}}{\varepsilon_0} = \frac{E_{\mathrm{ion}}}{E_\gamma} \ , \tag{5}$$

where E_γ is derived from the γ-ray energy calibration

and E_{ion} is evaluated using Eq. (2). Thus the response of the HPGe detector to energetic (i.e., few MeV) charged particles was derived *relative* to the response to γ rays.

III. RESULTS

Figure 1 shows portions of a typical 4096 channel spectrum for the triple-α source measured simultaneously with a ^{152}Eu γ-ray source. The energy of the calibrating γ ray in this case is 1.408 05 MeV. The two panels show the low- and high-energy regions: pulser peaks are positioned on both sides of all peaks of interest to provide a basis for linear interpolation, thereby yielding relative α and γ pulse heights. All measurements of relative pulse heights involved analyses of raw data similar to those illustrated in Fig. 1.

A. Nuclear energy loss

Considering the process of ionization by incident energetic particles in the depleted volume of semiconductor detectors, the electronic collisions (which are the dominant contributor to the projectile stopping) lead to electron-hole pair production. When a particle approaches the end of its range, nuclear collisions play a major role in the energy loss process, wherein the energy of the projectiles is transferred to target atoms by atomic scattering. The scattered target atoms (i.e., recoils) undergo a similar process as they slow down. The probability for those recoiling target atoms to create further ionization is quite small for the case of light incident ions, and thus a large fraction of the energy transferred to the detector atoms in elastic collisions does not lead to the production of electron-hole pairs. Therefore, the energy of an incident particle inferred only from the number of electron-hole pairs in the detector has to be corrected by the nonionizing part of the nuclear energy loss, which is one of the factors contributing to the pulse-height defect.

As an approximation, the nonionizing part of the nuclear energy loss for light ions in the Ge detector, ΔE_n, can be estimated via

$$\Delta E_n = \int_0^{E_0} dE_n = \int_0^R S_n dx = \int_0^{E_0} \frac{S_n}{S_n + S_e} dE \ , \qquad (6)$$

where R is the range of the incident particles in the detector material having an atomic density N and S_n is the nuclear stopping power. The total stopping values are derived from empirical stopping formulas.[14,15] The neglect of the ionizing effect caused by recoiling target atoms causes an overestimate of the correction for ΔE_n.

A second-order correction can be made by considering the energy loss of a primary recoil target atom through secondary recoils, i.e., the nuclear energy loss of Ge atoms in amorphous Ge. Assuming that the energy of the primary Ge recoil is T_r, the portion of T_r transferred by further nuclear collisions can be calculated[16] by

$$Q(T_r) = \frac{1}{T_r} \int_0^{T_r} \frac{S_n(E)}{S_e(E) + S_n(E)} dE \ . \qquad (7)$$

Then Eq. (6) can be modified to

$$\Delta E_n(E_0) = \int_0^{E_0} \frac{1}{S(E)} \int_0^{T_{\max}(E)} Q(T_r) T_r d\sigma(T_r, E) dE \ , \qquad (8)$$

where $T_{\max}(E)/E = 4M_1M_2/(M_1+M_2)^2$. The results should yield reliable estimates for ΔE_n, since the second-order correction represents $\leq 10\%$ of ΔE_n calculated us-

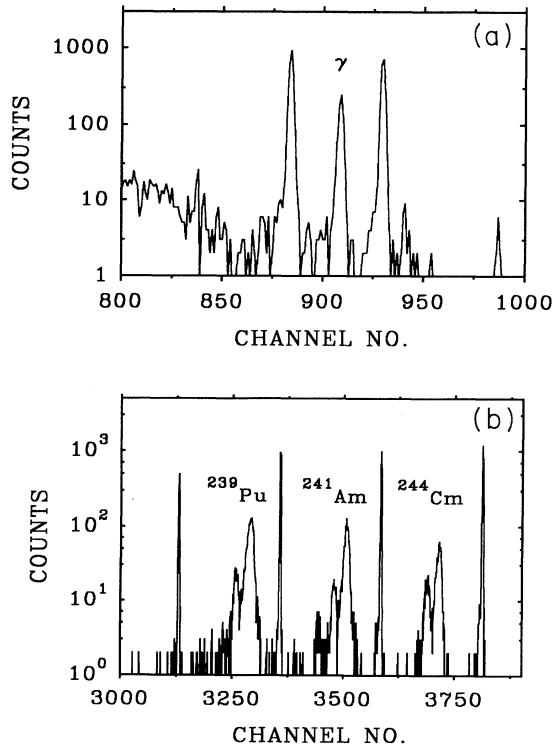

FIG. 1. Typical spectrum (for an α source) with pulser peaks, γ-peaks, and peaks due to α particles (5 MeV $< E_\alpha <$ 6 MeV): (a) low-energy region where $E_\gamma = 1.408\,05$ meV and (b) high-energy region.

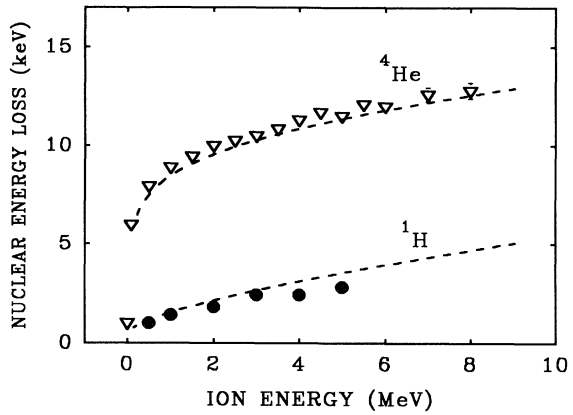

FIG. 2. Nuclear energy loss (ΔE_n) for ^{1}H and ^{4}He ions in Ge. The data points show values obtained using the TRIM program,[17] and the smooth curves are results calculated via Eq. (6).

ing Eq. (6). As a cross-check, the ΔE_n values were calculated by the TRIM Monte Carlo program.[17] All the data for ^{1}H and ^{4}He in Ge are shown in Fig. 2. The TRIM values are in reasonable agreement with those derived from calculations using Eq. (8). There are no experimental data available for comparison with the calculations.

B. Entrance window energy loss

Using the detector tilt method, viz. Eq. (1), the window energy loss for charged particles was measured for ^{1}H and ^{4}He at energies varying between 500 keV and a few MeV. Typical pulse-height data are shown in Fig. 3(a) for ^{1}H and Fig. 3(b) for ^{4}He. The two peaks in Fig. 3(b) are due to scattering from C ($\sim ch.$ 1165) and Au ($\sim ch.$ 1210) atoms; the narrow peaks originate from the precision pulse generator. At a few particular angles, the peak shapes showed structure on the high-energy side of the mean peaks: Fig. 4 shows such data for 0.5 MeV protons near $\theta=33°$ and Fig. 5 shows such data for 0.759 MeV ^{4}He ions near $\theta=6°$. The phenomenon responsible for such peak shapes is channeling, which for MeV light ions arises from a series of glancing (low-angle) collisions with lattice atoms; channeled projectiles encounter a lower than average electron density, causing a reduction in the electronic energy-loss rate. Since the slowing down arises mainly from electronic collisions, the energy deposited in the ion-implanted window region may be significantly smaller for ions parallel to low index crystallographic planes and/or axes than for those incident in a "random" direction. Note that for incident angles near

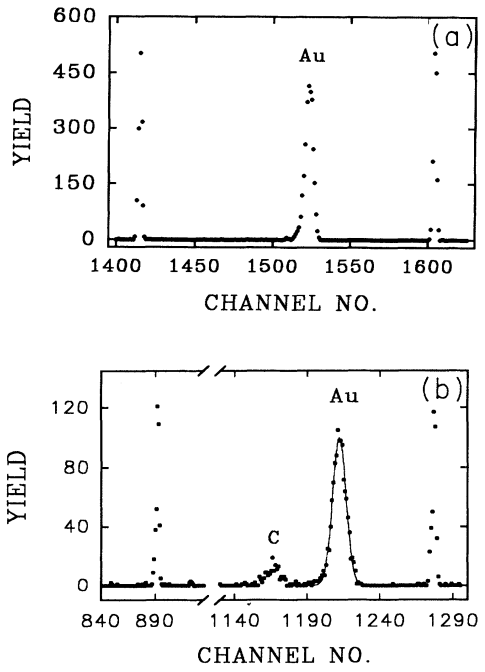

FIG. 3. Typical spectra observed for (a) ^{1}H ions at $E_0=2.0$ MeV scattered from a self-supporting Au thin foil target; and (b) ^{4}He ions at $E_0=1.98$ MeV scattered from a Au/C self-supporting thin foil target. The sharp peaks on either side represent those from the precision pulse generator.

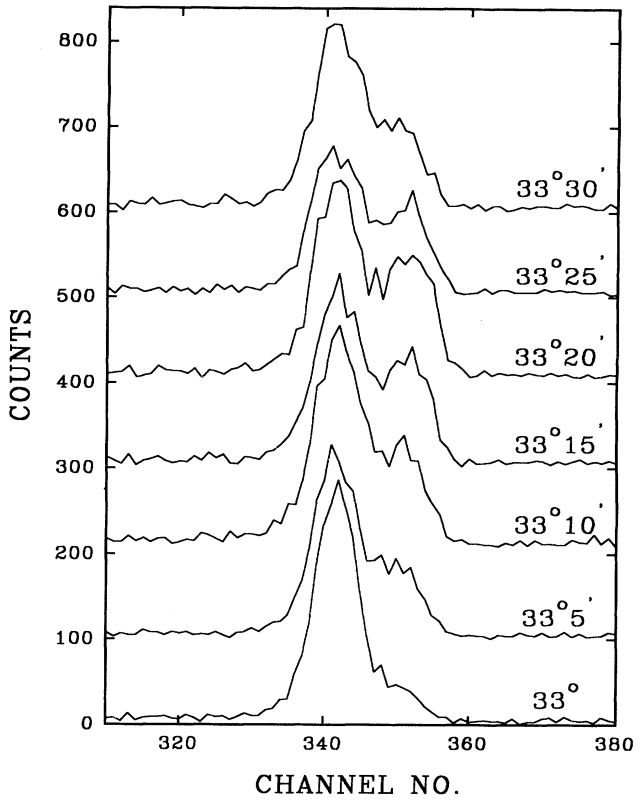

FIG. 4. Channeling effect observed in the Ge detector pulse-height spectra for incident 495 keV ^{1}H ions; the detector angle is shown (33°–33.5°) for each spectrum; there is a vertical offset for clarity.

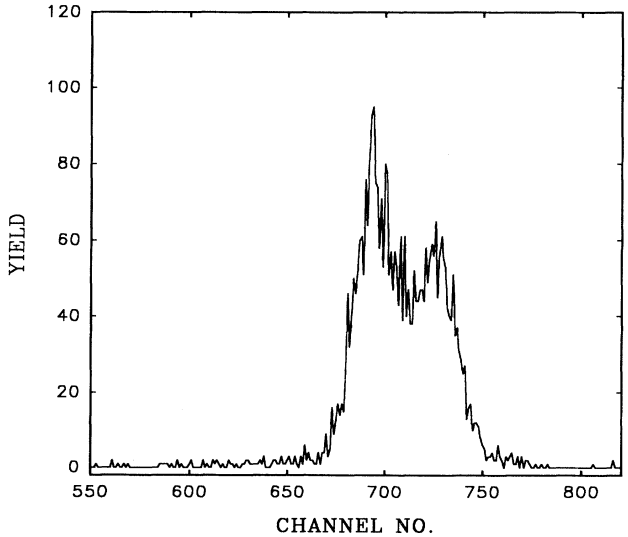

FIG. 5. Channeling effect observed in the Ge detector pulse-height spectrum for incident 759 keV ^{4}He ions [the scattering foil was a 10 μg cm^{-2} C foil for this measurement, to eliminate the double peaks such as those apparent in Fig. 3(b)]; the detector angle is 6.75° here.

the critical angle for channeling, the energy loss may *exceed* the random loss.

Further measurements for 1.48 MeV ^{4}He and 1.2 MeV ^{1}H ions were performed as follows.

(1) The pulse heights of the scattered protons and α particles were usually measured for detector tilt angles from $-47°$ to 45° in 2° increments (normal incidence corresponds to an incident angle $\theta_{\rm det}\sim -2.5°$ according to the rotary dial reading). The positions of those α peaks with high-energy shoulders were determined by fitting a Gaussian function with a low-energy exponential tail to the main part of the α peaks, excluding the high-energy shoulder; surprisingly, the results revealed structure on the tilting pulse height data wherein the measured pulse heights at some angles were significantly larger or smaller than expected; see Fig. 6 (increments of 1° for these data).

In Fig. 6, most of the pulse-height data follow the curve defined by Eq. (1). Since there is no prescription for defining the pulse heights for peaks with high-energy shoulders, those few data exhibiting channeling effects were initially excluded in the process of determining the fitting parameters via Eq. (1) for the window thickness. (The energy loss of the ions in channeling directions is different from the random value so that the measured pulse heights for channeled ions do not represent the random energy loss in the window layer.) However, even with the inclusion of these channeling data, the window thickness could still be determined with $\pm 1\%$ agreement with the value derived by excluding such channeling data. Additionally, with regard to channeling, a fit to *all* the tilt data should be appropriate since the parameter desired is the *average* energy loss in the window, which means averaging over all directions *including* those exhibiting channeling effects. In Fig. 6, the solid lines represent the fitted curves including the channeling data. The window energy loss was thus determined within $\pm 2\%$ for α's and $\pm 3-6\%$ for protons. We note that Grob, Grob, and Siffert[18] have already shown that the charge collection process is the same for both aligned and random penetration directions in Si. We make the reasonable assumption that such is the case for Ge as well.

(2) The pulse heights were measured in detail using small angular steps around those detector angles where structure was observed. Data for 0.759 MeV ^{4}He near $\theta=33°$ are shown in Fig. 7, where the scattering foil was changed to a 10 μg cm^{-2} carbon foil to eliminate the presence of the second Au peak. The angular dependence of these data confirmed the presence of channeling effects in the Ge detector window. The energy difference between the pulse heights for channeled and nonchanneled ions is too large to originate from any other source, e.g., the nonionizing energy loss. Additionally, the angular range over which the peak shapes exhibited significant structure corresponds closely to expected values for planar and axial channeling critical angles: specifically, the critical angles for ⟨100⟩ axial channeling in Ge are 0.88° for 0.8 MeV ^{4}He and 0.51° for 1.2 MeV ^{1}H ions;[19] smaller critical angles are expected for planar channeling.

Since the entrance window of the Ge detector was formed by implanting 40 keV ^{11}B ions into the surface of the Ge detector crystal to a total fluence of 10^{14} ions cm^{-2}, which would produce a $\sim 0.1-0.15$ μm thick boron-implanted surface layer *if the detector material were amorphous* Ge. However, the implantation dose was below the value necessary to amorphize the surface layer at $T=293$ K, i.e., the window layer retains a rather high

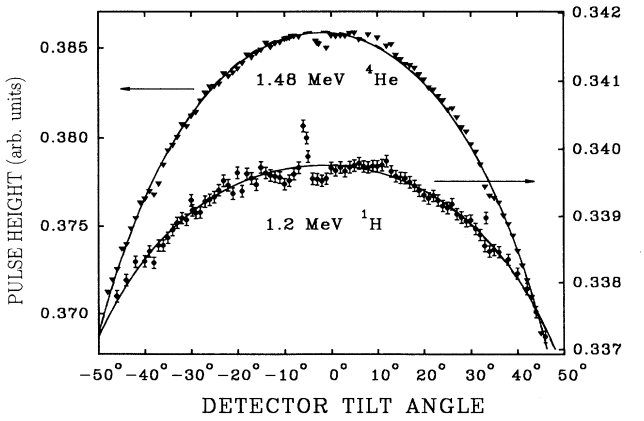

FIG. 6. Measured relative pulse height (PH) data as a function of the detector tilt angle (θ) for 1.20 MeV ^{1}H and 1.48 ^{4}He ions. The smooth curves result from a fit to *all* the data for each ion using the function $\mathrm{PH}=P_0-P_1\sec(\theta-\theta_0)$.

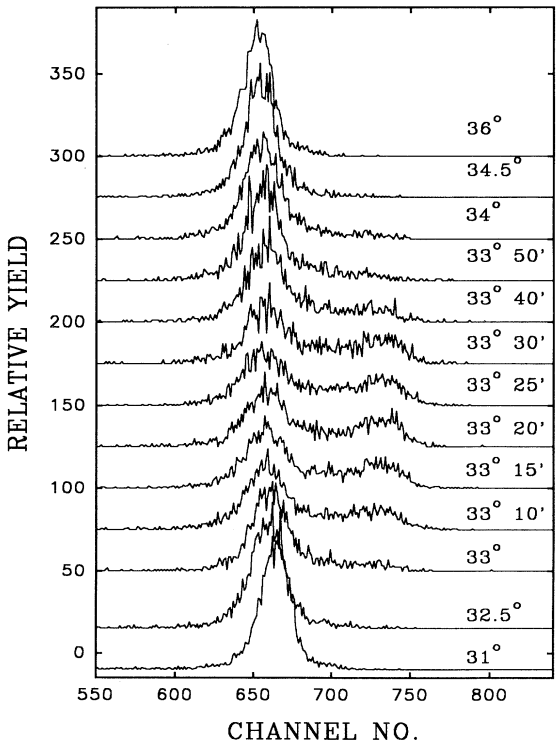

FIG. 7. Channeling effect observed in the Ge detector pulse-height spectrum for incident 759 keV ^{4}He ions scattered from a 10 μg cm^{-2} C foil for detector angles in the range 31°–36°. The spectra are offset vertically.

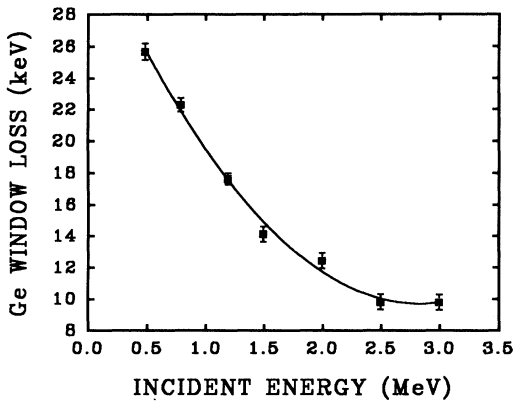

FIG. 8. Energy loss measured for ^{1}H ions in the window of the Ge detector at $T=80$ K as a function of the mean incident energy $E_p=E_0-\Delta E_w/2$. The curve is only a visual guide.

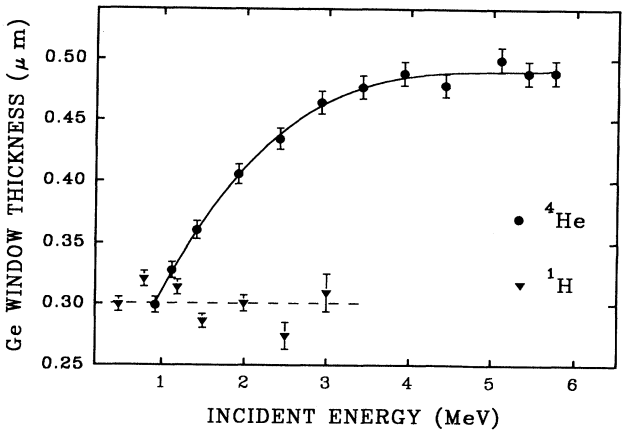

FIG. 10. Apparent thickness of the Ge detector window obtained from the data in Fig. 8 (^{1}H) and Fig. 9 (^{4}He), using stopping-power values from Refs. 14 and 15. The smooth curves are to guide the eye.

degree of crystallinity. Indeed, recent RBS-channeling studies of Ge(100) samples which were ^{11}B implanted (at room temperature) to a fluence of 10^{14} cm^{-2} at 40 keV showed no evidence for crystal damage in comparison to virgin Ge(100) samples, both for normal incidence and for 15° off-axis implantation directions.[20]

The dependence of the apparent Ge detector window thickness on incident particle energy was measured at 80 K for protons with energies in the range 0.5–3 MeV and for ^{4}He ions with energies in the range 1–4.5 MeV; see Figs. 8 and 9, respectively. The window energy losses obtained using both the ^{4}He beam and α sources were quite consistent, reaching a maximum near ~2.2 MeV. By dividing the measured energy loss values by the corresponding stopping power[14,15] at the appropriate projectile energy, the window loss was converted into an apparent Ge thickness; see Fig. 10. The derived window thickness for α's increases with particle energy and saturates in the region 4–5 MeV, while the window thickness derived for ^{1}H data has a value of 0.30 μm with ~10% fluctuations over the entire energy range 0.5–3 MeV. This observation suggests that the energy loss of α particles in the thin window layer is not simply proportional to the mean stopping power, which is difficult to understand based on the results from Ref. 1 where the energy loss of light ions in the Au window of Si surface-barrier detectors followed

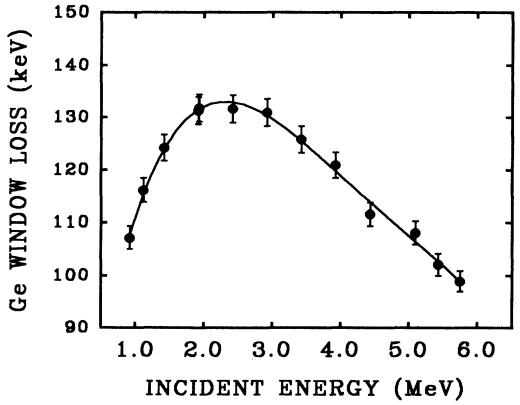

FIG. 9. Energy loss measured for ^{4}He ions in the window of the Ge detector at $T=80$ K as a function of the mean incident energy $E_\alpha=E_0-\Delta E_w/2$. The curve is only a visual guide.

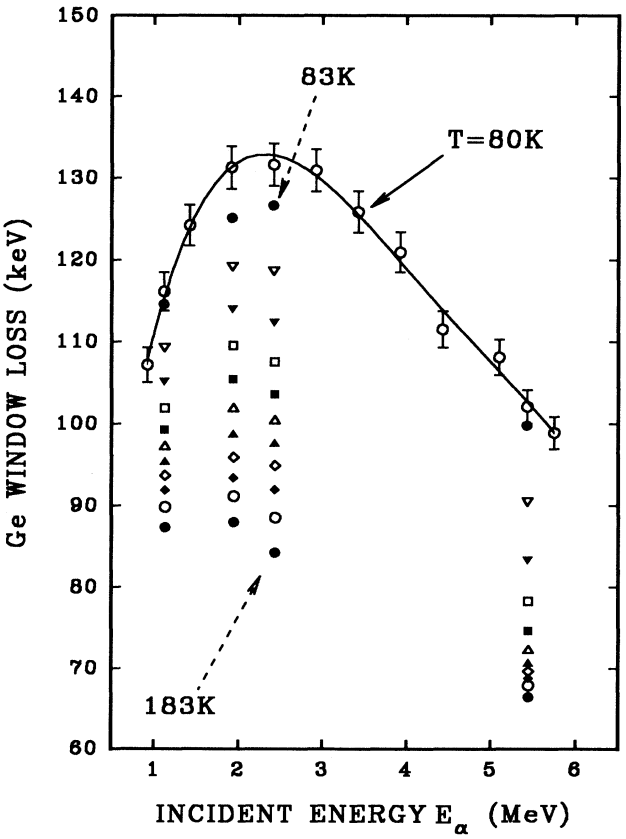

FIG. 11. Temperature dependence of the window energy loss measured for ^{4}He ions over the range 1 MeV $< E_\alpha <$ 5.5 MeV for the temperature region 80–183 K.

the corresponding stopping-power curve. Since the stopping-power maximum for protons in Ge is located near 100 keV, the window energy loss for a ^{1}H beam with $E > 500$ keV may have already saturated. All these data suggest that the window of the Ge detector may not be a simple conducting layer. The observed variable window energy loss represents the experimental evidence for such an effect.

Figure 11 shows the temperature dependence of the window energy loss measured for ^{4}He ions at three different energies (1.18, 2.48, and 5.48 MeV). We observe the following: first, the window energy loss changes dramatically with detector temperature, i.e., the window energy loss at 173 K was reduced to ~70% of this value at 80 K; secondly, the ^{4}He energy for which ΔE_w reaches its maximum value gradually shifts from ~2.2 MeV at 80 K to ~1.5 MeV at ~173 K, i.e., approaching the stopping maximum which occurs at $E_\alpha \approx 0.8$ MeV. Once again, the measurements suggest that the window is more complex than a simple conducting layer.

The window energy loss was measured for several values of bias voltage in the range 0.4–1.2 kV using incident 2.5 MeV ^{4}He ions. No change in the window energy loss was found with a variation in the applied bias voltage. This observation indicates that increasing the bias above the value required for total depletion does not cause the electric field to penetrate the window layer.

C. Ionization energy for charged particles in Ge

The energy of the incident ions before entering the Ge detector, E_0', was determined from the calibration of the Tandetron accelerator considering both the energy loss in the scattering foil (C/Au or Au) and the kinematic factor for scattering to 20°. After considering ΔE_w (and ΔE_s, if applicable) and ΔE_n, the effective energy of the incident ions contributing to the creation of electron-hole pairs on the Ge detector was calculated according to Eq. (2). For the radioactive source, ΔE_s was measured by tilting the α-emitting source with respect to the detector, yielding $\Delta E_s = 3.8 \pm 1.9$ keV for the three principal α groups. Since the number of electron-hole pairs is proportional to the measured pulse height, the ratio $\varepsilon_{\text{ion}}/\varepsilon_0$ is obtained directly using Eq. (5). ε_{ion} represents the average ionization energy at the energy E_{ion} [see Eq. (3)], and E_γ is the energy corresponding to the ion pulse height based on the calibration of γ-ray energy versus the γ pulse height measured simultaneously in the same spectrum. Again, as for the window energy loss, the pulse-height values at normal incidence derived in this manner were determined from ~40 measurements rather than from a single measurement.

Values of $\varepsilon_{\text{ion}}/\varepsilon_0$ were measured for the Ge detector at 80 K using a bias voltage of 1 kV. The results are shown in Figs. 12 and 13, and listed in Tables I and II, where E_γ is the γ-ray energy *corresponding to the same pulse height.* For protons, the Au self-supporting foil (68 μg cm^{-2}) was used; the C/Au (C: 11.2 μg cm^{-2}; Au: 9.6 μg cm^{-2}) self-supporting foil combination was used for ^{4}He ions.

The uncertainties for the incident energies shown in the first column of the tables arise from two sources: (1) the uncertainty in the energy calibration of the Tandetron accelerator; and (2) an estimated ±10% uncertainty in the measured thickness of the scattering foils. The former uncertainty reaches a minimum between the energies corresponding to the calibration energies and becomes larger for both lower and higher energies, while the latter one decreases with increasing energy (i.e., as the stopping power decreases).

The uncertainties arising from the window energy loss were taken to be ~2% for ^{4}He data and ~3–6 % for ^{1}H data, except for higher-energy ^{1}H data as discussed earlier. The uncertainties in ΔE_n values are difficult to estimate since they are based on calculations. For all cases, ±20% uncertainty in ΔE_n has been used in deriving an overall estimate for the uncertainty in $\varepsilon_{\text{ion}}/\varepsilon_0$, since the

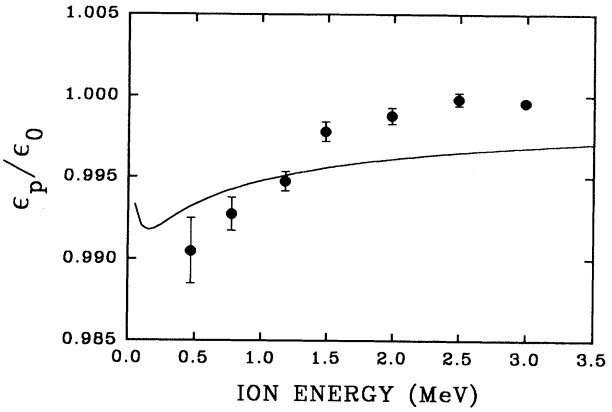

FIG. 12. Energy dependence of the ionization energy ratio, $\varepsilon_p/\varepsilon_0$, measured for ^{1}H ions at $T = 80$ K. The data are given in Table I. The solid curve shows the result obtained for Si detectors; see Ref. 1.

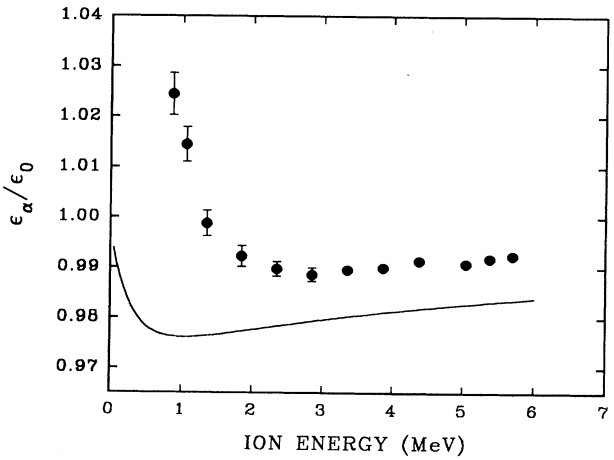

FIG. 13. Energy dependence of the ionization energy ratio, $\varepsilon_\alpha/\varepsilon_0$, measured for ^{4}He ions at $T = 80$ K. The data are given in Table II. The solid curve shows the result obtained for Si detectors; see Ref. 1.

TABLE I. Ionization energy ratio measured for ^{1}H ions in the HPGe detector at $T=80$ K. The values shown in column 5 for E_γ were derived from the analog-to-digital converter calibration measured simultaneously using a ^{152}Eu γ-ray source.

E_0 (keV)	ΔE_w (keV)	ΔE_n (keV)	E_{ion} (keV)	E_γ (keV)	$\varepsilon_{\text{ion}}/\varepsilon_0$
494.61±0.62	25.68±0.51	1.0	467.93±0.83	472.42±0.51	0.9905±0.0020
796.60±0.49	22.30±0.45	1.2	773.10±0.71	778.76±0.38	0.9927±0.0010
1197.60±0.40	17.64±0.65	1.4	1178.56±0.60	1187.77±0.47	0.9948±0.0006
1498.41±0.37	14.14±0.49	1.6	1482.67±0.69	1486.05±0.56	0.9978±0.0006
1999.72±0.34	12.44±0.50	1.8	1985.48±0.70	1987.90±0.86	0.9988±0.0005
2500.82±0.36	9.81±0.58	2.1	2488.91±0.80	2489.41±0.66	0.9998±0.0004
3001.41±0.39	9.79±0.59	2.4	2989.22±0.85	2990.47±0.54	0.9996±0.0003

differences in ΔE_n values calculated via different procedures is $\lesssim 20\%$; see Fig. 2.

In Figs. 12 and 13, the ionization energy ratios for ^{1}H and ^{4}He approach unity as the energy of the ion increases. The variation of $\varepsilon_p/\varepsilon_0$ and $\varepsilon_\alpha/\varepsilon_0$ with ion energy is qualitatively similar to results obtained for Si detectors: the solid curves in Figs. 12 and 13 show calculations assuming $\varepsilon_{\text{ion}}=\varepsilon_0-kS_e$ [where S_e is the electronic stopping power (i.e., $dE/dx>0$] for ^{1}H or ^{4}He ions in Ge). The value of k was taken to be the same as that determined empirically for Si,[1,2] viz. $k=2.8\times10^{-4}$ nm electron-hole pair. Obviously the rapid rise of $\varepsilon_\alpha/\varepsilon_0$ commences at an energy higher than that corresponding to the stopping-power maximum and the ratio exceeds unity for $E_\alpha<1.1$ MeV.

Figure 14 shows the dependence of $\varepsilon_\alpha/\varepsilon_0$ on the detector bias voltage for 2.48 MeV α's at 80 K. Based on a linear fit of $\varepsilon_\alpha/\varepsilon_0$ as a function of V_b^{-1}, the minimum value of $\varepsilon_\alpha/\varepsilon_0$ for 2.5 MeV α particles is 0.988 for an infinitely large electric-field value (i.e., $1/V_b\rightarrow0$). However, the actual value of $\varepsilon_\alpha/\varepsilon_0$ for $V_b\rightarrow\infty$ may be between 0.988 and 0.989 since the straight line extrapolation is only an estimate.

Regarding the T dependence of ε, $\varepsilon_0(T)$ was derived using ^{152}Eu, ^{60}Co, and ^{137}Cs γ sources over the temperature range 80–170 K. By adopting the value $\varepsilon_0=2.962$ eV electron-hole pair at 80 K (obtained by extrapolating the results of Ref. 5 from 90 to 80 K), the present relative results have been made absolute as shown in Fig. 15. The present data are in good agreement with those of Stuck *et al.*[21] Using the same normalization, $\varepsilon_\alpha(T)$ was determined at three E_α values. The results are shown in Fig. 16. The fractional difference between ε_α and ε_0 decreases as T increases. The solid curves in Fig. 16 show results that would be obtained for $\varepsilon_\alpha(T)$ if a *constant value* (corresponding to values measured at $T=80$ K) were assumed for ΔE_w. In that case, the $\varepsilon_\alpha(T)$ for 5.5 MeV α's and $\varepsilon_0(T)$ become exactly parallel (see Fig. 15).

Finally, Fig. 17 shows the bandgap (E_g) dependence of the ionization energy for α's and γ's in the Ge detector measured in this work. The linear dependence of ε_0 and E_g yields a slope of 1.934 and an intercept of 1.535 eV: both values agree with previous results[21] within 3%. $E_g(T)$ was taken from Ref. 22. However, a nonlinear change of ε_α with E_g is evident, particularly at low temperature. If a constant ΔE_w as a function of temperature were applied for measurements performed using ^{241}Am α particles, a linear relationship between ε_α and E_g would

TABLE II. Ionization energy ratio measured for ^{4}He ions in the HPGe detector at $T=80$ K. The values shown in column 5 for E_γ were derived from the analog-to-digital converter calibration measured simultaneously using a ^{152}Eu γ-ray source. ($\Delta E_s=3.8\pm1.9$ keV).

E_0' (keV)	ΔE_w (keV)	ΔE_n (keV)	E_{ion} (keV)	E_γ (keV)	$\varepsilon_{\text{ion}}/\varepsilon_0$
976.1±2.3	107.2±1.6	8.6	860.3±3.2	839.8±1.6	1.0245±0.0042
1176.9±2.0	116.2±1.7	9.1	1051.6±3.2	1036.7±1.9	1.0145±0.0034
1478.5±1.8	124.2±1.9	9.4	1344.9±3.2	1346.6±1.7	0.9987±0.0025
1981.3±1.6	131.3±2.0	10.0	1840.0±3.2	1854.4±2.0	0.9923±0.0021
2482.7±1.2	131.6±2.0	10.2	2340.9±3.2	2365.1±1.9	0.9898±0.0015
2984.3±1.6	130.9±2.0	10.5	2842.9±3.1	2875.6±2.2	0.9886±0.0014
3485.0±1.5	125.8±1.9	10.8	3348.4±3.3	3383.5±1.8	0.9896±0.0011
3985.8±1.7	120.9±1.8	11.2	3853.7±3.2	3892.6±1.9	0.9900±0.0010
4486.5±2.0	111.6±1.7	11.5	4363.4±3.5	4401.2±1.7	0.9914±0.0009
$5156.6-\Delta E_s$	108.1±2.2	11.6	5033.1±3.7	5079.5±2.0	0.9908±0.0010
$5485.6-\Delta E_s$	102.1±1.5	11.9	5367.8±3.4	5412.0±2.1	0.9918±0.0010
$5804.8-\Delta E_s$	98.9±2.0	12.2	5689.9±3.7	5733.5±2.3	0.9924±0.0010

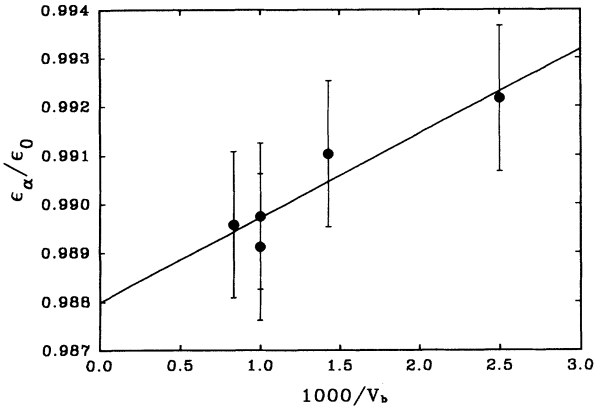

FIG. 14. Bias voltage dependence of $\varepsilon_\alpha/\varepsilon_0$ measured for 2.483 MeV ^{4}He ions at $T=80$ K (V_b: units of volts). The solid line is a linear fit to the data.

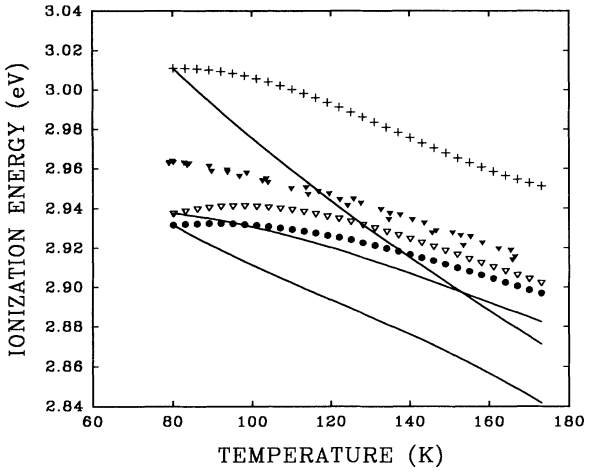

FIG. 16. Temperature dependence of measured values for ε_0 and ε_α. ▽: ε_α (5.486 MeV); ●: ε_α (2.483 MeV); +: ε_α (1.177 MeV); ▼: ε_0 (^{137}Cs, ^{152}Eu). See text for an explanation of the solid curves.

be obtained here (see also Refs. 5, 21, and 23). Stuck *et al.*[21] have asserted that ε has almost always been observed to change linearly with E_g in both Si and Ge. Theoretical descriptions[24–26] predict a linear relation for all semiconductors, although the slope of the ε vs E_g function is not always the same. Thus the present data for ε_α should be regarded circumspectly in light of the puzzling behavior of the detector window thickness as a function of temperature.

IV. DISCUSSION

According to the manufacturer, the Ge crystal was cut nearly parallel to the (100) plane. Since the critical angle for 40 keV boron ions channeling in the ⟨100⟩ axial direction of a Ge crystal is ~7°, it is likely that channeling occurred during the boron implantation process. Therefore, the range of implanted boron ions will undoubtedly exceed the value calculated for amorphous Ge. Carrier-concentration measurements[27,28] for 20 keV boron implantation (10^{14} ions cm^{-2}) in the ⟨111⟩ and ⟨110⟩ directions of a Ge crystal shows a flat and high-charge carrier concentration, ~10^{18} cm^{-3}, up to depths ~0.35 and ~0.6 μm, respectively. These depths exceed the expected projected range for amorphous Ge by a factor of 4–5. This observation, together with a consideration of the present results for the apparent window thickness of the Ge detector (see Fig. 10), demonstrates that the boron distribution must extend to depths larger than the 0.1 μm value predicted by TRIM[17]—i.e., the "random" range. However, it is difficult to estimate the boron penetration for the channeling case. However, the proton data shown in Fig. 10 seem to indicate a window thickness ~0.3 μm.

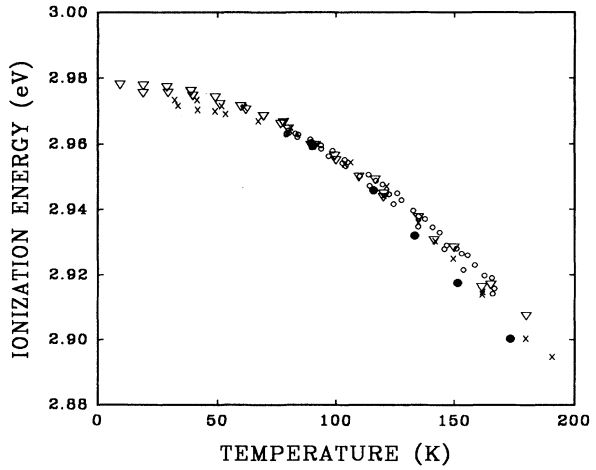

FIG. 15. Temperature dependence of ε measured here compared to earlier results. ○: ε_0, this work using ^{137}Cs and ^{152}Eu γ sources; ▽: ε_α, Ref. 21; ×: ε_0, Ref. 21; ●: $\varepsilon_{0,\alpha}$, Ref. 5.

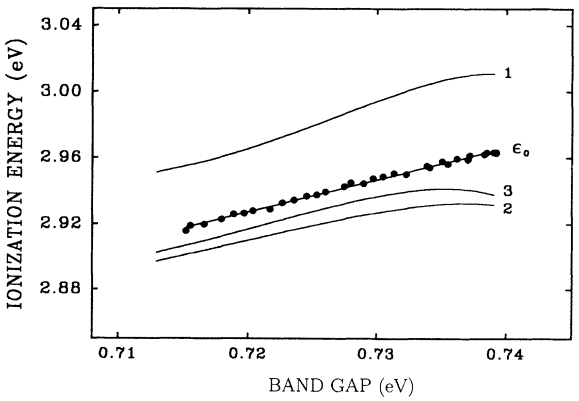

FIG. 17. Ionization energy for γ rays and ^{4}He ions as a function of the band gap. The straight line is a fit to the ε_0 data. The data marked by 1, 2, and 3 correspond to $E_\alpha=1.177$, 2.483, and 5.486 MeV, respectively.

Since energy-loss straggling in the window region is the dominating contributor to the detector resolution for incident ^{4}He ions, then the resolution should improve if the window layer thickness actually decreases with increasing temperature. The electronic energy loss straggling (modification of the Bohr formula) is given by

$$\Omega_e^2(E)=f(E)4\pi Z_1^2 Z_2 e^4 \Delta t \ , \tag{9}$$

where Δt is the window thickness, Z_1 and Z_2 are the atomic numbers of the incident ion and target atom, respectively, and $f(E)$ (≤ 1) is derived from Ref. 29. The FWHM is obtained by FWHM$=2.3548\Omega_e$. For measurements, the FWHM must be corrected for the electronic noise. (Energy-loss straggling for α particles in the C/Au scattering foil is insignificant here; e.g., $\sim$2 keV.) Figure 18 shows measurements of the temperature dependence of FWHM values for 2.48 MeV α particles. The smooth curve shows the calculated FWHM values using the data shown in Fig. 11: the energy loss has been divided by the ^{4}He stopping power and Eq. (9) used to calculate Ω_e. The change in the measured straggling FWHM is similar to that expected based on measurements of $\Delta E_w(T)$; see Fig. 11. Thus the detector resolution data suggest that the change in the apparent window thickness with the Ge crystal temperature may be caused by a variation of its physical thickness with temperature. Note that this technique has almost always been used, e.g., by Pehl *et al.*[5] and Herzer *et al.*,[27] to estimate the detector entrance window thickness. Since the origin of the measured ^{4}He energy dependence of ΔE_w as shown in Fig. 11 (and in Fig. 9) remains an open question, one may not make definitive statements concerning the actual physical thickness of the window region.

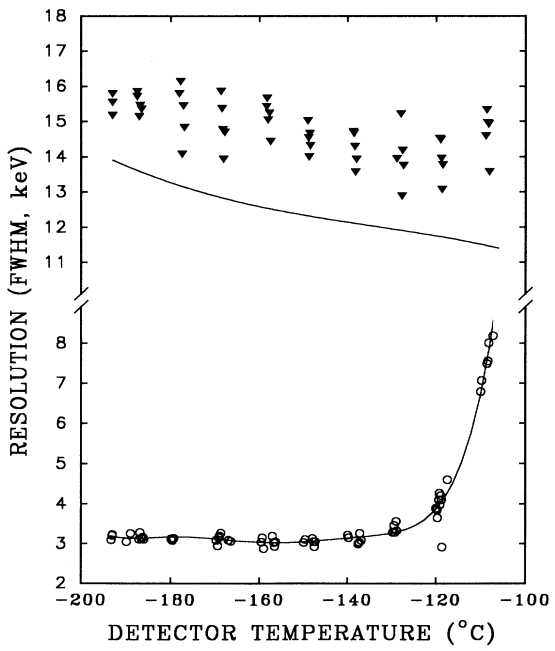

FIG. 18. Temperature dependence of measured FWHM values (i.e., resolution) for 2.483 MeV ^{4}He ions: the open circles show FWHM values for test pulses and the solid triangles show measured FWHM values. The origin of the smooth curve is given in the text.

The decrease of the apparent window thickness with increasing temperature suggests the presence of charge trapping during the course of carrier transportation. In principle, trapping effects will be reduced at higher temperature because of a shorter carrier detrapping time.[30] However, there is no evidence of a trapping effect for protons and γ rays. Since the charge carriers travel approximately the same distance when detecting both ^{1}H and ^{4}He ions, then trapping would appear to be unlikely.

If we assume (at $T=80$ K) that $\varepsilon_p \equiv \varepsilon_0$ for $E_p > 3$ MeV (see Table I and Fig. 12) and that $\varepsilon_\alpha \equiv \varepsilon_0$ for $E_\alpha > 5.8$ MeV (see Table II and Fig. 13), then we can predict a value for $\varepsilon_\alpha/\varepsilon_p$ at 15 MeV using Eq. (3) via

$$\frac{\varepsilon_p(15\ \text{MeV})}{\varepsilon_\alpha(15\ \text{MeV})}=\frac{3[\varepsilon_p(3\ \text{MeV})/\varepsilon_0]+(15-3)}{5.8[\varepsilon_\alpha(5.8\ \text{MeV})/\varepsilon_0]+(15-5.8)} \ . \tag{10}$$

Using the values $\varepsilon_p/\varepsilon_0=0.9996\pm0.0003$ (Table I, $E_p=3$ MeV) and $\varepsilon_\alpha/\varepsilon_0=0.9924\pm0.0010$ (Table II, $E_\alpha=5.8$ MeV), we find $\varepsilon_\alpha/\varepsilon_p=0.9971\pm0.0004$ at 15 MeV. Martini's data[6] show reasonable agreement with this prediction for 10–19 MeV ^{1}H and ^{4}He particles in a Ge detector at 90 K, i.e., their results yield $\varepsilon_\alpha/\varepsilon_p=0.9989\pm0.0015$. Specifically, their measured $\varepsilon_\alpha/\varepsilon_p$ ratio has approximately the same magnitude as predicted here and is in the *same* direction.

With regard to carrier recombination and trapping effects, we see in Fig. 14 only a small variation of ε_α with the bias for voltages $\gtrsim 1$ kV. It is recognized that the plasma density of electron-hole pairs is higher for ^{4}He ions than for γ rays or ^{1}H ions, which can increase recombination of electron-hole pairs created by the passage of a charged particle. We have also observed highly symmetric line shapes for $\sim$5.5 MeV α's, which is usually evidence for complete charge collection.[31] In principle, a large electric field in the detector should reduce effects arising from recombination, especially for ions. For γ rays, no recombination effects are expected for sufficiently high-bias voltages. We conclude that any residual recombination and/or trapping effects for bias voltages exceeding 1 kV can contribute at *most* 0.0015 to the derived ionization energy ratio, $\varepsilon_{\text{ion}}/\varepsilon_0$. (Even for infinitely large electric fields, recombination cannot always be completely eliminated since the penetration of the electric field into the electron-hole pair plasma may be limited.) Note that charge trapping and recombination effects for ions will always act to *increase* the measured value of $\varepsilon_{\text{ion}}/\varepsilon_0$.

Additionally, any dependence of γ and α pulse heights on detector bias are not likely caused by a charge-carrier multiplication effect, which requires a minimum electric field of $\sim 10^6$ V cm^{-1} in semiconductor detectors,[30] i.e., much larger than the value ($\sim 10^3$ V/cm) used here. If charge multiplication were occurring in the detector, a high-energy tail in the peaks should be detected for monoenergetic radiation; such tails have not been observed.

In previous studies[5,6] of the ionization energy for α's in Ge detectors, a constant window thickness (in terms of *physical length)* as a function of T was always assumed for boron-implanted Ge detectors and all α particle energies exceeded 5 MeV, so that the temperature dependence of ε_α always mirrored that of ε_0. We have shown that the previous result for $\varepsilon_\alpha(T)$ (Ref. 21) can be reproduced here by making the same assumption (for ~ 5 MeV α's).

Comparing Ge and Si detectors, we find that the largest difference in ε values for light ions and γ rays in Ge is $\sim 1\%$ at 80 K; as expected, this difference approaches zero as the particle energy increases which is to be expected based on the similarity between the electromagnetic fields of fast charged particles and photons (method of virtual quanta). In conjunction with this observation, we note that $\varepsilon_{e^-} = \varepsilon_0$ has always been confirmed. The latter result provides convincing evidence that systematic errors in the measurements have been avoided. The energy dependence of $\varepsilon_{\text{ion}}/\varepsilon_0$ for ^{1}H and ^{4}He ions in Ge exhibits a similar trend with that found for Si detectors.

Contrary to earlier published data for Si and Ge detectors, ε_{ion} in the Ge detector shows a nonlinear dependence on E_g; see Fig. 17. The temperature dependence of the detector window energy loss is an important contributor in producing such a nonlinear effect. Measurements of the effective window thicknesses of the boron-implanted Ge detector, based on the tilting technique, have shown that the (ion-implanted) window thickness can be estimated from a measurement of the energy-loss straggling. This observation raises a question concerning the window correction for ε values measured in Si detectors. It is not clear how the window thickness of Si detectors was measured as a function of temperature in Ref. 5. It is possible that the temperature dependence of the window thickness could be large enough to alter the linear dependence of ε_{ion} on E_g for Si, despite the fact that the measured window energy losses (at $T = 293$ K) in previous studies[1,5] were quite small (e.g., 0.5% effect on ε_α).

V. CONCLUSIONS

Summarizing the results from the experimental studies performed here, we conclude the following.

(1) There is an $\sim 1\%$ difference between ε_{ion} (light ions at low energy) and ε_0, often exhibiting $\varepsilon_{\text{ion}} < \varepsilon_0$. This conclusion *cannot* be attributed to trapping or recombination effects during the stopping of the ion in the sensitive volume—both of which would act *in the opposite direction* to yield a result $\varepsilon_{\text{ion}} > \varepsilon_0$. This conclusion is contrary to the results found from earlier investigations, where large experimental uncertainties precluded the measurement of such small effects with sufficient precision.

(2) For very energetic ions, $\varepsilon_{\text{ion}} = \varepsilon_0$, as expected.

(3) The apparent window thickness measured for the detector under study varies with (i) incident particle type, (ii) ion energy, and (iii) detector temperature in a manner that suggests that this ^{11}B ion-implanted surface layer does not consist of a simple passive inactive layer. The origin of this behavior remains an open question.

(4) Where comparisons can be made with earlier works, the present results for $\varepsilon_{\text{ion}}/\varepsilon_0$ are in quantitative agreement when similar assumptions are adopted, e.g., when we assume that the apparent window thickness does *not* depend on temperature.

(5) The observed behavior for Ge is in qualitative, but not quantitative, agreement with that of Si detectors.

(6) Channeling effects for the incident ions as they traverse the ion-implanted entrance window region are readily observed; however, such effects are *not* responsible for the intrinsic deviations of the $\varepsilon_{\text{ion}}/\varepsilon_0$ ratio from unity.

We believe that the present investigation represents the most comprehensive attempt until now to determine precise relative ε values for Ge. Further measurements should concentrate on an intensive study of the ion-implanted window region, i.e., $\varepsilon_\alpha/\varepsilon_0$ should be determined using different conditions (implant dose and energy) for fabricating the ^{11}B-implanted front contact. As well, the detector crystal should be cut *off-axis* to produce two beneficial advantages: (i) channeling effects for both ^{11}B implantation and particle detection would be minimized, and (ii) the value of ΔE_w would be substantially reduced for all particle types, since the implanted region should be much thinner for random incidence angles during boron implantation. This remark is motivated by the unexplained behavior observed for the energy loss of ions, specifically ^{4}He ions, transmitted through the front contact as a function of ion energy and temperature. Finally, future measurements using charged particles might benefit from the use of a Ge detector with a smaller depletion depth to minimize effects due to both carrier recombination and trapping. However, this advantage will yield a concomitant decrease in γ-ray detection efficiency for simultaneous particle-γ pulse-height measurements.

ACKNOWLEDGMENTS

The technical support of J. Hendricks, S. Brawn, D. F. O'Dacre, and H. Chen was much appreciated. The authors wish to acknowledge stimulating discussions with I. V. Mitchell, L. C. Feldman, J. A. Davies, A. Dygo, and G. F. Knoll. This research was made possible through grants from the Natural Sciences and Engineering Research Council (NSERC) of Canada.

*Present address: Department of Physics, McMaster University, Hamilton, Ontario, Canada L8S 4M1.

[1] W. N. Lennard, H. Geissel, K. B. Winterbon, D. Phillips, T. K. Alexander, and J. S. Forster, Nucl. Instrum. Methods Phys. Res. A **248**, 454 (1986).

[2] P. Bauer and G. Bortels, Nucl. Instrum. Methods Phys. Res. A **299**, 205 (1990).

[3] W. Hösler and R. Darji, Nucl. Instrum. Methods Phys. Res. B

85, 602 (1994).
[4]D. Comedi and J. A. Davies, Nucl. Instrum. Methods Phys. Res. B **67**, 93 (1992).
[5]R. H. Pehl, F. S. Goulding, D. A. Landis, and M. Lenzlinger, Nucl. Instrum. Methods **59**, 45 (1968).
[6]M. Martini, T. W. Raudorf, W. R. Stott, and J. C. Waddington, IEEE Trans. Nucl. Sci. **NS-22**, 145 (1973).
[7]A. Rytz, At. Data Nucl. Data Tables **23**, 507 (1979).
[8]F. S. Goulding and D. A. Landis, in *Nuclear Spectroscopy and Reactions,* edited by J. Cerny (Academic, New York, 1974).
[9]H. R. Bilger, Phys. Rev. **163**, 238 (1967).
[10]F. S. Goulding and D. A. Landis, IEEE Trans. Nucl. Sci. **NS-35**, 119 (1988).
[11]A. J. Levy and R. C. Ritter, Nucl. Instrum. Methods **49**, 359 (1967).
[12]J. B. Marion, Rev. Mod. Phys. **38**, 323 (1966).
[13]J. A. Leavitt, L. C. McIntyre, Jr., P. Stoss, J. G. Oder, M. D. Ashbaugh, B. Dezfouly-Arjomandy, Z. M. Yang, and Z. Lin, Nucl. Instrum. Methods Phys. Res. B **40/41**, 776 (1989).
[14]H. H. Andersen and J. F. Ziegler, *Hydrogen: Stopping Power and Ranges in All Elements* (Pergamon, New York, 1977), Vol. 3.
[15]J. F. Zielger, *Helium: Stopping Powers and Ranges in All Elements* (Ref. 14), Vol. 4.
[16]E. L. Haines and A. B. Whitehead, Rev. Sci. Instrum. **37**, 2 (1966).
[17]J. F. Ziegler, J. P. Biersack, and U. Littmark, *The Stopping and Range of Ions in Solids* (Pergamon, New York, 1985), Vol. 1.
[18]A. Grob, J. J. Grob, and P. Siffert, Nucl. Instrum. Methods **132**, 273 (1976).
[19]D. S. Gemmell, Rev. Mod. Phys. **46**, 129 (1974).
[20]H. Xia (private communication).
[21]R. Stuck, J. P. Ponpon, R. Berger, and P. Siffert, Rad. Effects **20**, 75 (1973).
[22]G. G. Macfarlane, T. P. McLean, J. E. Quarrington, and V. Roberts, Phys. Rev. **108**, 1377 (1957).
[23]C. Canali, M. Martini, G. Ottaviani, and A. Alberigi Quaranta, IEEE Trans. Nucl. Sci. **NS-19**, 9 (1972).
[24]C. A. Klein, J. Appl. Phys. **39**, 2029 (1968).
[25]W. Shockley, Czech, J. Phys. B **11**, 81 (1961).
[26]E. Antončik, Rad. Effects **7**, 275 (1971).
[27]H. Herzer, S. Kalbitzer, J. P. Ponpon, R. Stuck, and P. Siffert, Nucl. Instrum. Methods **101**, 31 (1972).
[28]H. Herzer and S. Kalbitzer, in *Proceedings of the 2nd International Conference on Ion Implantation in Semiconductors, Garmisch-Partenkirchen,* edited by I. Ruge and J. Graul (Springer, Berlin, 1971), p. 307.
[29]J. W. Mayer and E. Rimini, *Ion Beam Handbook for Material Analysis* (Academic, New York, 1977).
[30]G. F. Knoll, *Radiation Detection and Measurement,* 2nd ed. (Wiley, New York, 1989).
[31]S. Kalbitzer (unpublished).